GEOPHYSICS, VOL. 56, NO. 9 (SEPTEMBER 1991); P. 1349–1364, 22 FIGS.

Changes in shear-wave polarization azimuth with depth in Cymric and Railroad Gap oil fields

D. F. Winterstein* and M. A. Meadows*

ABSTRACT

Shear-wave (*S*-wave) polarization azimuths, although consistent over large depth intervals, changed abruptly and by large amounts at various depths in nine-component vertical seismic profiling (VSP) data from the Cymric and Railroad Gap oil fields of the southwest San Joaquin basin. A simple layer-stripping technique made it possible to follow the polarization changes and determine the *S*-wave birefringence over successive depth intervals. Because the birefringence and polarization azimuth are related to in-situ stresses and fractures, information from such analysis could be important for reservoir development.

Near offset VSP data from Cymric indicated that the subsurface could be approximated roughly as two anisotropic layers. The upper layer, from the surface to 800 ft (240 m), had vertical *S*-wave birefringence as large as 14 percent. Vertical birefringence in the lower layer was about 6 percent down to 1300 ft (400 m). In the upper layer the polarization azimuth of the fast *S*-wave was N 60°E, while in the lower layer it was about N 10°E. Refinement of the layer stripping showed that neither layer was anisotropically homogeneous, and both could be subdivided into thinner layers.

Near offset S-wave VSP data from the Railroad Gap well also show high birefringence near the surface and less birefringence deeper. In the uppermost layer, which extends down to 1300 ft (400 m), the *S*-wave birefringence was 9 percent, and the lag between the fast and slow *S*-waves exceeded 60 ms at the bottom of the layer. Seven layers in all were needed to accommodate *S*-wave polarization changes. The most reliable azimuth angle determinations as judged from data consistency were those of the uppermost layer, at N 46°E, and those from depths 2900–3700 ft (880–1130 m) and 3900–5300 ft (1190–1610 m), at N 16°E and N 15°W, respectively. Over those intervals the scatter of calculated azimuths about the mean was typically less than 4 degrees.

The largest birefringence at both locations occurred in the same formations, the Pliocene Tulare sands and Pebble Conglomerate. In those formations the azimuth of the fast *S*-wave polarization was roughly orthogonal to the San Andreas fault that lies about 10 mi (16 km) to the southwest. In the deeper Antelope shale, *S*-wave polarization directions in both areas were close to 45 degrees from the fault.

Confidence in the layer stripping procedure was bolstered by major improvements in data quality that resulted from stripping. Before stripping, wavelets of the two *S*-waves sometimes had very different waveforms, and it was often impossible to come close to diagonalizing the 2 × 2 *S*-wave data matrix by rotating sources and receivers by the same angle. After stripping, wavelets were more similar in shape, and the *S*-wave matrix was more nearly diagonalizable by rotating with a single angle.

INTRODUCTION

This paper's primary contributions are that it documents major changes in *S*-wave polarization azimuth with depth in VSP wells of two oil fields, and it illustrates how a simple layer stripping process makes it possible to follow and study such changes. The paper also shows that layer stripping can be successfully applied to sparsely sampled offset VSP data. A further contribution is the documentation of large vertical *S*-wave birefringence in near surface formations, up to 14 percent to a depth of 800 ft (240 m) in Cymric and about 9 percent to a depth of 1300 ft (400 m) in Railroad Gap. A companion paper (Winterstein and Meadows, 1991; herein-

Presented at the 60th Annual International Meeting, San Francisco, CA. Manuscript received by the Editor October 9, 1990; revised manuscript received March 19, 1991.
*Chevron Oil Field Research Company, 1300 Beach Blvd., P.O. Box 446, La Habra, CA 90633-0446.

after called Paper I) discusses concepts and procedures, including layer stripping, in greater detail than this paper and may be consulted for background information and further introductory material.

Lefeuvre et al. (1989) and Cox et al (1989) used propagator matrices or transfer functions instead of layer stripping to analyze variations in *S*-wave birefringence with depth in multicomponent VSP data. Both the transfer function method and the layer stripping method seem well suited to the purpose, but this paper does not compare the two methods. *S*-wave birefringence effects shown here, especially changes in *S*-wave polarization direction with depth, are significantly larger and better defined than they were in data shown in those two papers. At this early stage in the recording and analysis of such effects, it is important for credibility and for deducing causes to document obvious effects like those shown here.

Results presented here cannot be correlated as confidently with horizontal stress directions as those of Paper I because independent evidence for stress orientations is less compelling. Available evidence at Cymric, however, including offset VSP information presented here, supports the notion that the vertical *S*-wave birefringence is caused by horizontal stresses, and that the polarization direction of the fast *S*-wave lies in the direction of maximum horizontal compressive stress, even when subsurface structures are steeply dipping. At Railroad Gap there are significant discrepancies between fast *S*-wave polarization directions and stress directions obtained from differential strain curve analysis (DSCA), but the latter may be unreliable (see Discussion). The proximity of the San Andreas fault [10 mi (16 km) to the southwest] adds to the plausibility that *S*-wave polarization directions are controlled by contemporary stresses rather than by fractures or other structures unrelated to those stresses. It is possible and even likely, however, that rocks exist for which the polarization direction of the fast *S*-wave for vertical travel does not lie along the maximum horizontal stress direction. Rocks with fractures oriented by ancient stress regimes, or rocks of low symmetry with tilted symmetry axes, for example, might constrain the fast *S*-wave polarization to lie in a direction other than that of maximum horizontal stress.

This paper shows unmistakable evidence for major changes in *S*-wave polarization direction with depth (see also Martin et al., 1986). A relationship between these polarization changes and any change of horizontal stress direction certainly exists, and the *S*-wave birefringence data provide potentially useful information for reservoir development regardless what the relationship is; but more study is needed, at least at Railroad Gap, to find that relationship.

The comment of Paper I on terminology is appropriate here. The term "polarization" in the context of seismic waves refers to the shape and spatial orientation of particle trajectories. Here we restrict the term to mean only the spatial orientation of the line along which a particle moves in a linearly polarized wave.

DATA ACQUISITION AND CONDITIONING

Data sets to be discussed in detail were from nine-component VSPs recorded in one well each of the Cymric and Railroad Gap oil fields in the southwest San Joaquin basin of California. The wells were about 4.5 mi (7.2 km) apart. By nine-component data we mean records from three orthogonal receiver components that detected waves as if from three separate, orthogonal source polarizations (Figure 1 of Paper I). In this paper, except for preliminary processing involving vertical components, we treat only data of the 2 × 2 *S*-wave data matrix, that is, data from *x* and *y* sources and receivers, or four of the nine components. Our coordinate frame for recording and processing was a right-handed Cartesian frame with the *x*-axis along a source vehicle axis; after data analysis the frame was oriented relative to true north. The locations of the two oil fields relative to the Lost Hills field and nearby fields in Kern and San Luis Obispo counties are shown in Figure 2 of Paper I.

Cymric VSP

We used a single ARIS™ source for the near offset portion of the VSP and alternated between two ARIS sources for three rings of offset VSPs and a walkaway VSP. For near offset recording, the ARIS was 77 ft (23 m) north of the well. Because of the hole deviation (see below), the source was suitably placed for vertical raypaths in the near offset VSP. For offset recording, we positioned the sources successively at eight points nominally 45 degrees apart in each of three concentric rings nominally 200, 325, and 700 ft (60, 100, and 210 m) of horizontal distance from the 1550 ft (472 m) level of the well. The walkaway VSP was along a north-south road near the VSP well. Each source position was marked with two 14 in. (0.36 m) rebar pegs whose positions were subsequently surveyed for accurate source locations and azimuths. For near offset recording, we built a special ARIS baseplate pad of road base gravel to do all recording without moving the source. We found it important for the layer stripping process not to move the source (see Paper I). For offset recording, no pads were needed because source effort at a given position was small. ARIS made 20 impacts per receiver level or offset position, five in each of four directions—fore, aft, left, and right—with the impactor tilted 15 degrees from the vertical. The source vehicle axis pointed towards the well at every source location. Source zero-times were obtained from pulses from an accelerometer atop the impactor that were transmitted to the recording truck via hard-wire connection.

The downhole receiver was the LRS-1300 3-C tool with the Gyrodata gyrocompass attached. We recorded the near offset VSP at increments of 50 ft (15 m) from a depth of 1550 ft (472 m) up to 100 ft (30 m). For the two outer rings of offset VSPs and the walkaway VSP, the receiver was at a fixed depth of 1550 ft (472 m), while for the inner ring of offset VSPs the receiver was at 1000 ft (305 m).

Railroad Gap VSP

Sources, receivers, and experimental procedures were the same as those used at Cymric, but receiver depths, depth increments, and source offsets differed. For the near offset VSP, the ARIS was 64 ft (20 m) SSW of the well. For offset recording, we positioned the sources successively at eight points nominally 45 degrees apart and 1000 ft (300 m) from the wellhead. Because of the complexity of the *S*-wave

polarization changes with depth, we have not interpreted the Railroad Gap offset data and do not discuss them here. For the near offset VSP the receiver levels ranged from 6500 to 100 ft (1981 to 30 m) in 200 ft (61 m) increments, while for the offset VSPs the receiver was clamped at 5500 ft (1676 m).

Wells and topography

The VSP wells were both new wells that were cased and cemented but not perforated. The Cymric well, the 1610S of section 1-30S/21E, had a constant rate of deviation slightly east of north, which displaced the well bottom 125 ft (38 m) north of the wellhead. The Railroad Gap well, the 355 of section 15-30S/22E, was nonuniformly deviated a maximum of about 53 ft (16 m) to the south and 150 ft (46 m) to the east, with the 6500 ft (1981 m) level about 13 ft (4 m) south and 150 ft (46 m) east of the wellhead. The fluid level was lowered in each well to about 300 ft (90 m) to prevent tube waves, which were undetectable.

In both fields, there was considerable surface relief; differences in offset source elevations exceeded 80 ft (25 m) at Cymric and 120 ft (37 m) at Railroad Gap. The relief caused irregularities in offset VSP source spacing but was not a major problem because numerous flat and compacted roads and well pads were available.

Data conditioning

Data conditioning steps were identical to those described in Paper I.

METHODS AND MODELS

The objective of data analysis was to quantify subsurface *S*-wave birefringence or, in other words, to find the natural polarization directions of the two *S*-waves and the time delays or lags between them. The purpose of quantifying birefringence is to correlate birefringence effects with formation properties such as direction of maximum horizontal stress. Figure 3 of Paper I illustrates in simplest terms our experiment and basic model.

Symmetry axis of the medium

For arbitrary ray directions in anisotropic rocks of low symmetry, one needs a great deal of information to interpret *S*-wave time lags and polarizations. However, if the rocks have vertical two-fold symmetry axes, analysis is straightforward if raypaths are vertical, and polarization directions relate in simple ways to symmetries of the rocks. Our initial assumption was that the rocks had vertical two-fold axes and that symmetry properties did not change with depth. Hence we positioned the near offset sources so as to get raypaths as close to vertical as possible. The purpose of the offset and walkaway VSPs was to evaluate the assumption of vertical symmetry axes and test robustness of polarization analyses done on vertical ray data.

Polarization analysis

The natural polarization direction of the subsurface rock is the angle at which *S*-wave energy on off-diagonal components of the 2 × 2 *S*-wave data matrix becomes a minimum (Alford, 1986), a criterion we call the "Alford rotation" criterion (see Paper I).

Layer stripping

We had expected *S*-wave polarizations to remain constant with depth, but data analysis showed that they did not. Polarization changes at Cymric and Railroad Gap were large and unmistakable, and we developed a layer stripping method specifically to analyze them. Layer stripping involves simply subtracting anisotropy effects in a layer in order to analyze anisotropy effects in the layer immediately below. If polarization varies with depth, polarization analysis will be confused if there is no compensation for the variation. Paper I discusses details of layer stripping concepts, procedure, how to choose layer boundaries, etc.

RESULTS

Cymric near offset VSP data

The near offset traces of Cymric VSP data are shown in Figure 1 after rotating receivers into alignment with the source. Figure 2 shows the same data after rotation to minimize energy on the off-diagonal components in the analysis window indicated. Within the analysis window, wave amplitudes on the off-diagonal components are small down to about 800 ft (240 m) but increase progressively below that level. This progressive increase indicates failure of the overly simple model and is a sign that *S*-wave polarization directions changed significantly below 800 ft (240 m).

Initial rotation analyses gave *S*-wave polarization azimuths that were nearly constant, at about N 60°E, down to about 1100 ft (330 m); below that level azimuths increased about 10 degrees (Figure 3a). Lag rose rapidly and almost

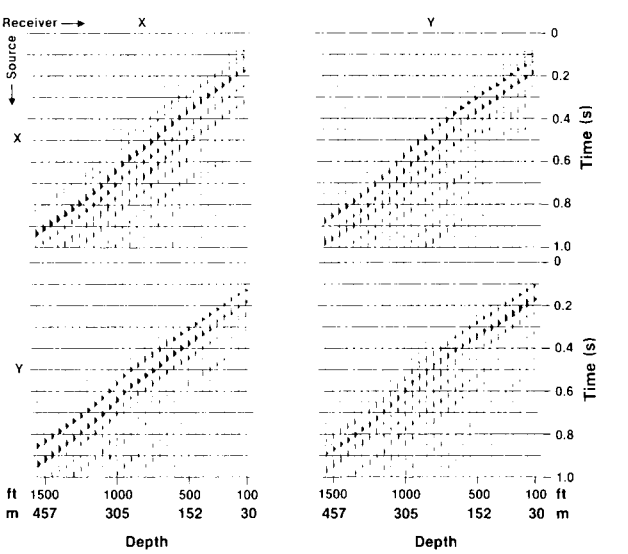

FIG. 1. 2 × 2 *S*-wave data matrix from the Cymric VSP after aligning receivers with sources but before Alford rotations. If the subsurface had been isotropic with horizontal layering, no signal would have appeared on off-diagonal (XY and YX) components.

linearly down to about 800 ft (240 m) and then decreased slowly (Figure 3b). The plateau in the lag curve from 100–350 ft (30–110 m) may result partly from horizontal components of raypath; the azimuth angles in that depth zone are constant and consistent with those below 350 ft (110 m). The decline in *S*-wave lags below about 800 ft (240 m) indicates a significant change in birefringence. The only way lags can diminish as they do, when the ray direction is constant, is for anisotropy to change; hence trends in the lags indicate a boundary for layer stripping between 800–850 ft (240–260 m). Note that the presence of a boundary at 800 ft (240 m) is not evident in azimuth angle trends (Figure 3a), an illustration of the effect of inertia in azimuth angle determinations below a highly birefringent layer (see Paper I). Refined layer stripping (below) shows that shallow changes in azimuth are completely masked by this inertia effect.

Layer stripping down to 800 ft (240 m) and then performing Alford rotation analysis showed that, below 800 ft (240 m), the azimuth angles were essentially constant at N 60°E plus 40°, or N 100°E (i.e., N 80°W—shown as circles in Figure 4). The lags as calculated were negative, however, indicating that N 80°W is the azimuth of the slow wave; hence, under the assumption of orthogonal *S*-wave polarizations, the fast *S*-wave is at N 10°E. The lag after layer stripping increased linearly by 12 ms between 1000 and 1300 ft (300 and 400 m) (Figure 5), a change not evident in data before stripping (Figure 3b). Two anomalous plateaus remain in the lag curve after stripping (Figure 5), one at 850–950 ft (260–290 m), the second at 1350–1550 ft (410–470 m). Both of these vanished after refining the layer stripping. Results of the initial *S*-wave birefringence analyses from the surface to 1550 ft (470 m) are summarized in Figures 6 and 7.

We note that Yardley and Crampin (1990) analyzed synthetic data based on the two-layer model implied by Figures 6 and 7 and got results almost identical to those of Figure 3. Their work thus supports our layer stripping procedure and results.

Figures 6 and 7 show results from layer stripping at only one level, where there were obvious cues in the data that layer stripping was needed. What if there were other polarization changes not signaled so obviously by a change in the lag curve? A change in polarization azimuth of 10–20 degrees, for example, might have little effect on the shape of the lag curve. To evaluate the possibility that the anisotropy might not be as simple as the initial analysis indicated, we layer stripped arbitrarily at levels 400, 450, and 500 ft (122, 137, and 152 m) (Figure 8). If the polarization directions had been constant in the upper layer as Figure 6 suggests, then azimuth angles after such arbitrary layer stripping should be the same as before. Figure 8 shows instead a systematic, large change in the angles, while the lags (not shown) were practically unaffected. As illustrated in Paper I, polarization directions from layer stripping are sensitive to the amount of lag used in stripping; hence the angles of Figure 8 cannot be

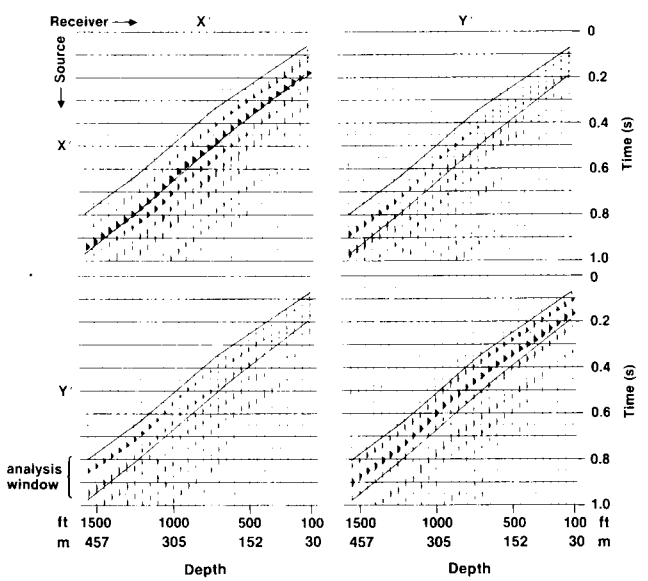

FIG. 2. Data of Figure 1 after Alford rotations but no layer stripping. Energy of off-diagonal components is small in the analysis window above 800 ft (240 m). Rotation in this case was by the complement of the calculated angle, causing Y'Y' arrivals to come in ahead of X'X'.

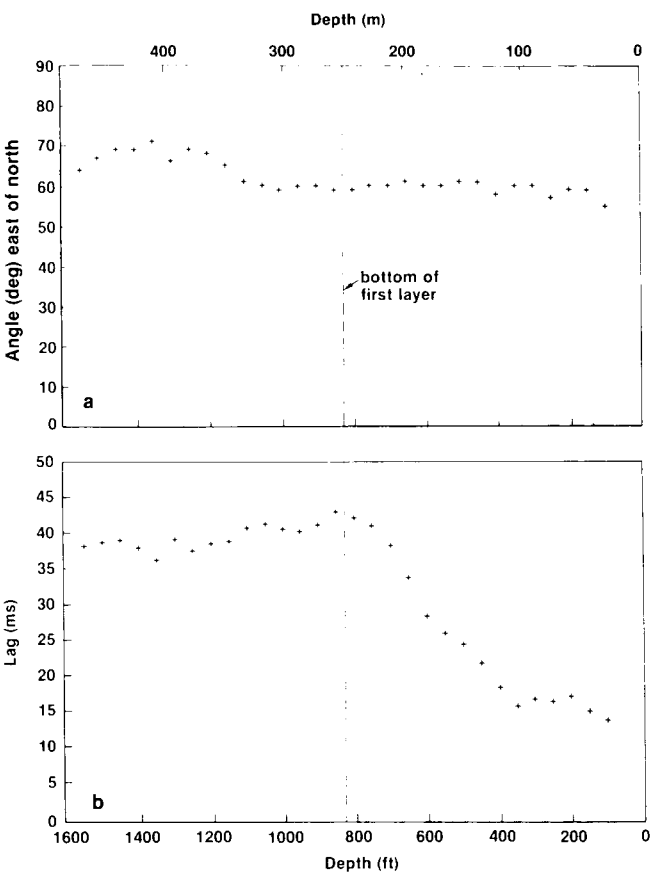

FIG. 3. a) Polarization azimuths of the fast *S*-wave as determined from the initial Alford rotation analysis of Cymric VSP data before any layer stripping. Angles are very consistent down to 1100 ft (330 m). b) Lags between *S*-waves of the Cymric VSP after the initial Alford rotation analysis but before any layer stripping. Above 800 ft (240 m) the *S*-wave birefringence reaches 14 percent. The abrupt change of slope near 800 ft (240 m) signals a major change in *S*-wave polarization, detected by layer stripping and subsequent Alford rotation analysis.

taken at face value. But the large discrepancies from the original angles indicated a need for more refined layer stripping.

The fine layer stripping ran into immediate difficulties. The original lags of the first five levels (Figure 3b) were anomalous because of the large lag at the very first level and relatively little change at subsequent levels. This behavior may result partly from the change in incidence angle near the surface. In any case, none of our many attempts at fine layer stripping gave consistently increasing lags between 100–600 ft (30–183 m), so on the basis of layer stripping criteria, that zone was effectively isotropic. However, because of the change in incidence angle we could not assume that layer stripping was handling those anomalous points well. Consequently, we did the fine layer stripping with two different sets of initial angles and statics, not knowing which was more correct, in order to test a range of possibilities. The results are shown in Figures 9 and 10. The points shown as triangles had an initial rotation angle of 60 degrees and a 15.2 ms static shift. Points shown as circles had a combination of a 60-degree rotation and 13.6 ms static followed by a 20-degree rotation and 2.5 ms static.

Except near the unconformity at 975 ft (297 m) and in the opal CT zone at 1450–1500 ft (440–460 m) the azimuth angles

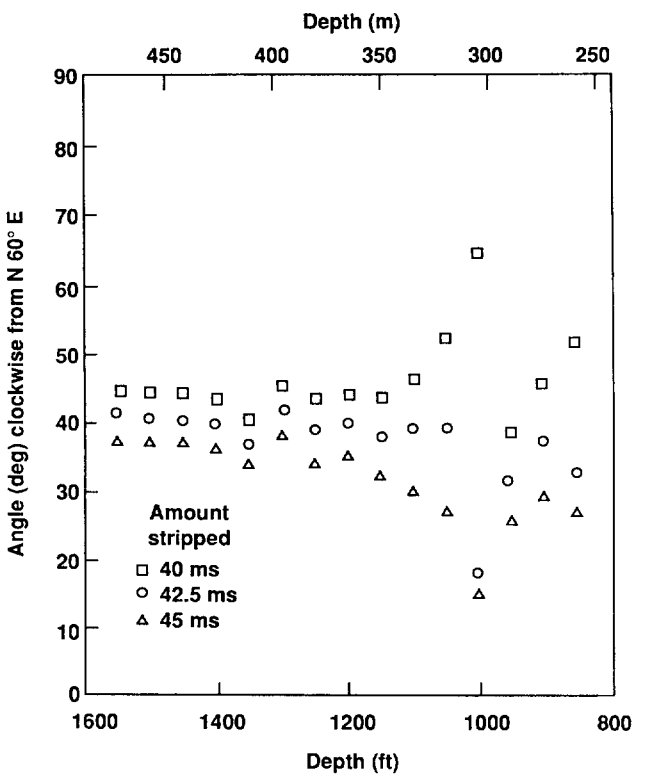

FIG. 4. Polarization azimuths of the Cymric VSP slow *S*-wave after layer stripping with three different statics: the best value, 42.5 ms, and test values of 40 and 45 ms. Angles are shown relative to N 60°E, the rotation angle applied to all data before layer stripping. Angles agree well at the greater depths but less so near the unconformity at 975 ft (300 m). The point at 1000 ft (305 m) is clearly not trustworthy in this layer stripping attempt.

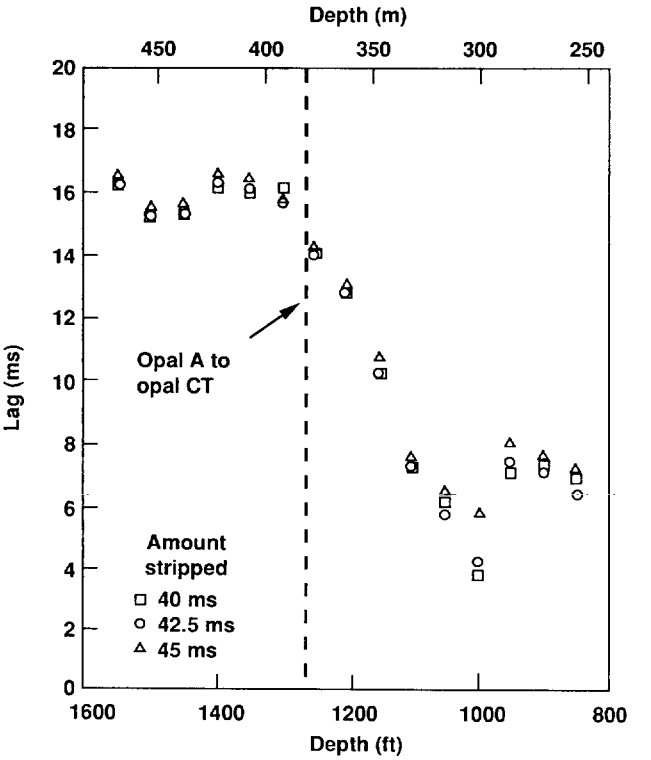

FIG. 5. Lags between *S*-waves of the Cymric VSP after layer stripping with three different statics: the best value, 42.5 ms, and test values of 40 and 45 ms. The lag after stripping was insensitive to the layer stripping static. Layer stripping over thinner intervals eliminated the lag anomaly above 1000 ft (305 m).

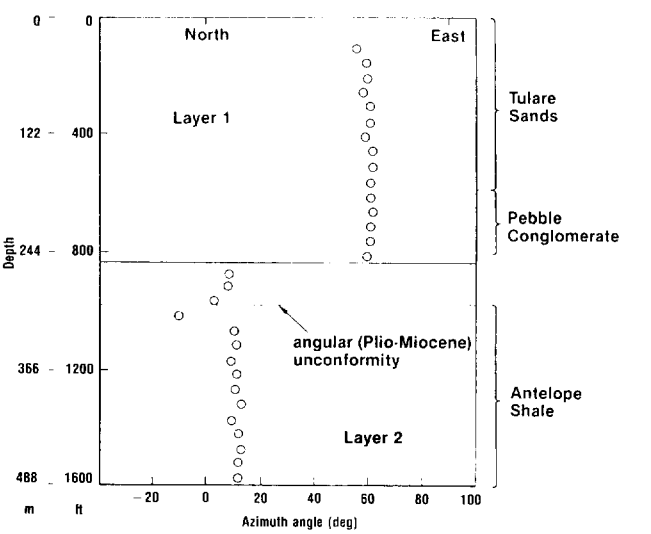

FIG. 6. Summary of polarization angles of the fast *S*-wave versus depth for the Cymric VSP data under the two-layer assumption. Consistency is very high for both layers.

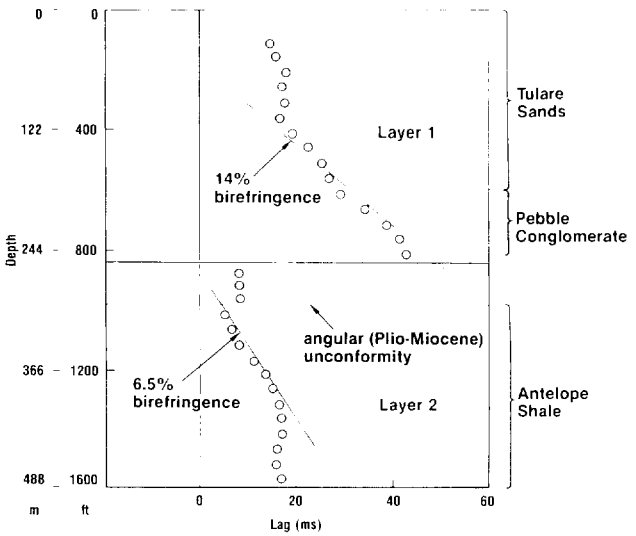

FIG. 7. Summary of *S*-wave lag versus depth for the Cymric VSP data under the two-layer assumption. Vertical *S*-wave birefringence was unusually large in Layer 1 and in a portion of Layer 2.

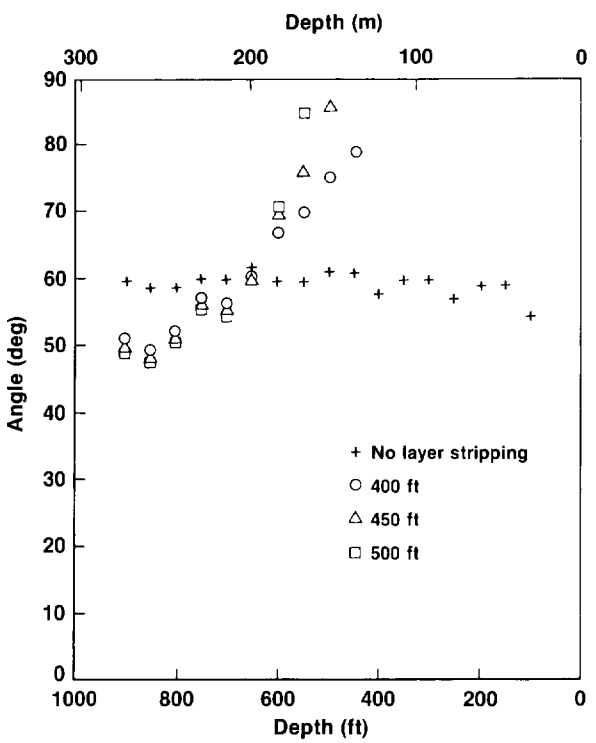

FIG. 8. *S*-wave polarization angles from layer stripping arbitrarily at 400, 450, and 500 ft (122, 137, and 152 m). The plusses show the angles obtained by Alford rotation analysis but no layer stripping (see Figure 6). The discrepancies between those angles and the ones from arbitrary layer stripping indicate that Layer 1 of Figure 6 is not anisotropically homogeneous but should be subdivided into thinner layers. The lags obtained by this arbitrary layer stripping were practically indistinguishable from those of Layer 1 of Figure 7 at corresponding depths.

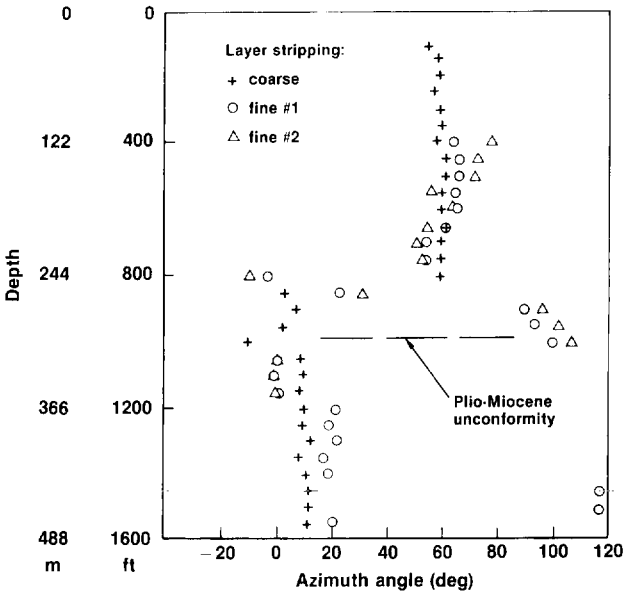

FIG. 9. *S*-wave polarization angles from two sequences of fine layer stripping. Two separate sequences were explored because it was not possible from the data to determine an unambiguous starting point. Except near the unconformity and near the deepest levels, the azimuth angles closely resemble those obtained under the two-layer assumption (Figure 6). Below 1150 ft (350 m) the azimuths from the two fine layer strippings converged.

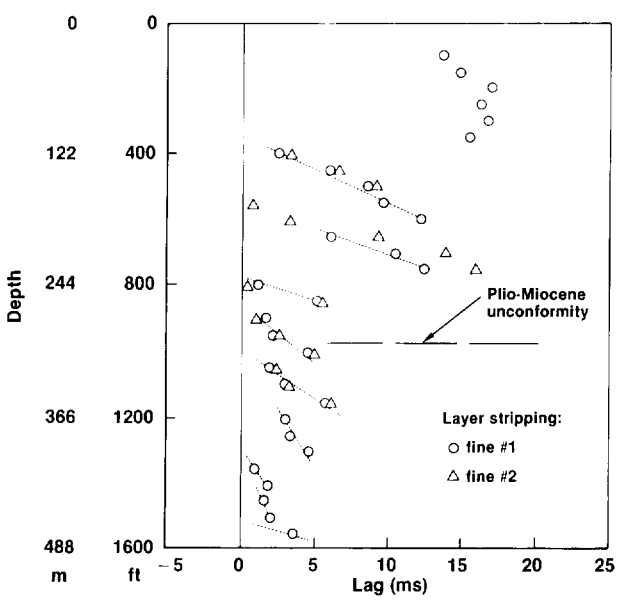

FIG. 10. *S*-wave lags from the two sequences of fine layer stripping shown in Figure 9. Lags in every layer increase monotonically in accord with layer stripping model assumptions. Below 1150 ft (350 m) the lags from the two fine layer strippings converged.

of the fine layer stripping are close to those from the initial analysis; but systematic discrepancies appear. The large discrepancies near the unconformity are probably significant because the trends in lags are well established (Figure 10): also, the initial layer stripping produced angles and lags there that did not fit the two-layer model (Figures 6 and 7). The large discrepancy at 1450–1500 ft (440–460 m) is not as believable because of the small lags. Below 1150 ft (350 m) the answers from the two fine layer strippings converged. It is clear from the fine layer strippings that the constancy of azimuth angle (Figure 6) is only apparent and results from the inertia effect.

Although anisotropy structure is not as simple as the initial analyses indicated, there are still two principal zones, an upper zone, where fast *S*-wave polarizations average roughly N 60°E, and a lower zone, where they average roughly N 10°E. Near the unconformity is a third zone where polarizations vary rapidly and are not consistent with those of other zones.

As a check on layer stripping, it is useful to monitor VSP traces closely after each stripping to determine whether the results fit layer stripping models. Figure 11 compares off-diagonal components at the deepest levels before and after the initial (two-layer) stripping. According to the model, amplitudes of the *S*-wave direct arrivals on off-diagonal components should be zero after Alford rotations. Figure 11 shows that they are clearly lower after layer stripping than before. A more subtle effect worth noting is that the leading edges of the diagonal *S*-wave wavelets are more similar after layer stripping than before (Figure 12), consistent with expectations from simple models. Comparable improvement in data did not result from the fine layer stripping at the deepest levels [at and below 1400 ft (427 m)]. This suggests that repeated layer stripping over small intervals can hurt data quality. Nevertheless, for reasons given above, we believe that the fine layer stripping gives a more accurate picture than layer stripping under the two-layer assumption.

Cymric offset VSP data

The outer rings.—Cymric offset VSP data with receiver at the 1550 ft (472 m) level give moderately consistent *S*-wave polarization azimuths (Figure 13), but the large birefringence of the upper zone dominates. That is, most azimuths are closer to N 60°E than to N 10°E. This is understandable in view of Figure 7, which shows that the total lag for the lower zone from the initial layer stripping is only about half that of the upper zone and hence insufficient to overcome the effect of the upper zone. Also, Figure 3a shows that, for near offset data in the absence of layer stripping, the deeper zone had minimal effect on the azimuth angle calculated at 1550 ft (472 m).

The offset data at Cymric are important because of steep structural dip, about 35 degrees to the southwest, below the Plio-Miocene unconformity that occurs at about 975 ft (300 m). If symmetry properties were to dip in the same way as bedding, the polarization directions determined from near offset data might depend in complicated ways on in-situ stress directions and hence could not be interpreted without more information (see Figure 14; also Figure 5 of Paper I). However, modeling suggests that, if *S*-wave polarizations in offset data were all similarly oriented, the symmetry properties of the subsurface would be such as to allow straightforward interpretation of polarization azimuths. Hence the offset data were to serve as either a warning against or encouragement for straightforward interpretation.

Therefore we had a strong incentive to determine polarization directions of the deeper zone from offset VSP data. Layer stripping worked well for the near offset data and seemed worth a try for the offset data. We implemented it

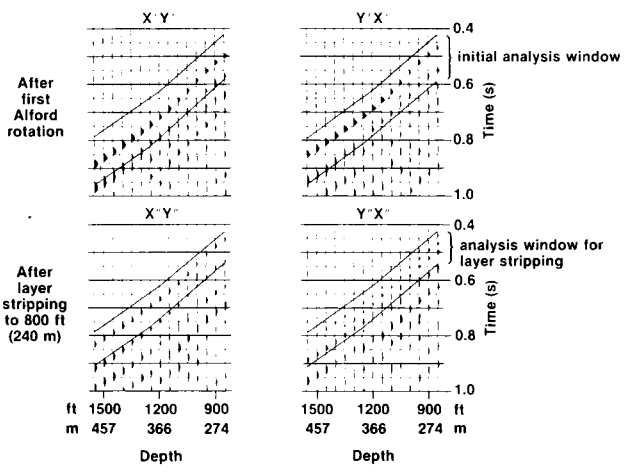

FIG. 11. Off-diagonal components of the 2 × 2 *S*-wave data matrix from the Cymric lower zone after the first Alford rotation (upper plots) and after the initial layer stripping to 800 ft (240 m) (lower plots). In the analysis window, signal amplitudes are lower after layer stripping (bottom) than before (top), an indication that layer stripping caused a better fit to the seismic model.

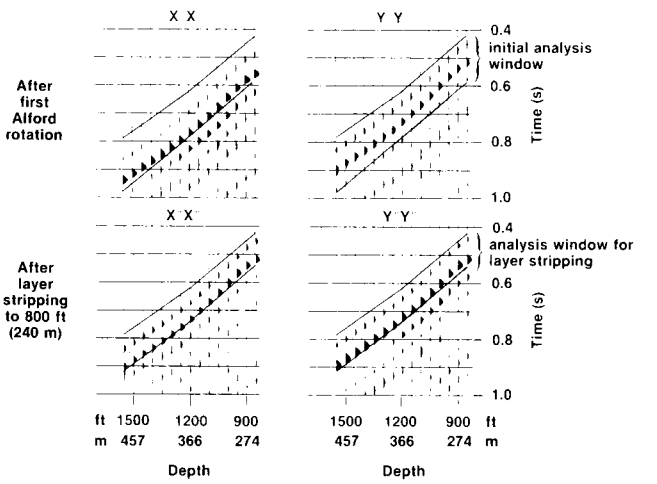

FIG. 12. Diagonal components of the 2 × 2 *S*-wave data matrix from the Cymric lower zone after the first Alford rotation (upper plots) and after the initial layer stripping to 800 ft (240 m) (lower plots). In the analysis window, leading portions of wavelets on XX components are more similar to their counterparts on YY components after layer stripping (bottom) than before layer stripping (top), an indication that layer stripping caused a better fit to the seismic model.

initially by rotating source and receiver x-axes along N 60°E, the fast S-wave polarization direction, and applying a 42.5 ms static to the y' source data, just as for the near offset data. Results of Alford rotation analysis were not encouraging; polarization directions had wide scatter and little discernable pattern.

The problem was that the initial time delay between the two S-waves—that is, the time delay after the initial Alford rotation analysis—varied strongly with source location. Because polarizations determined after layer stripping are sensitive to the amount of lag used in stripping, we had to decide whether the lag variation originated in the upper zone and, if so, whether to remove its effects by stripping off the variable lags. We decided the lag variations originated in the upper zone for the following reasons: First, the upper zone was highly birefringent, so that a relatively small percentage change in birefringence could lead to appreciable changes in lag. Also, near surface layers are generally more variable than deeper layers, and the offset VSP raypaths are maximally separated at the surface. The large separation would tend to make S-waves experience maximal near surface variability. Raypath segments in the lower zone, in contrast, were closer together because they were converging on the receiver and hence less likely to encounter significant variability. Furthermore, the near offset data show little change in lag below 800 ft (240 m) before layer stripping (Figure 3b), because the S-wave polarization directions of the lower zone are intermediate between the fast and slow directions of the upper zone. That is, if fast S-wave polarization directions remained the same in both zones, lag would increase in accord with the full birefringence of the lower zone; if polarizations changed by 90 degrees, lag would decrease a like amount; but if polarizations changed by 45 degrees, lag would tend to remain constant.

We accomplished the final offset VSP layer stripping by rotating all source and receiver x-axes along N 60°E, calculating lags of S-waves on diagonal components of the 2 × 2 S-wave data matrix for each source location, and then subtracting the different lags from the corresponding y' source data. Alford rotation analysis after layer stripping with the individually tailored lags gave polarizations that were remarkably consistent (Figure 15) in view of all the assumptions; the mean azimuth angle was 10.1 degrees and the standard deviation 12.7 degrees. The consistency of the answers partly justifies the assumptions but, more importantly, indicates that the fast S-wave polarization directions in zero-offset data may be interpreted straightforwardly. Specifically, because of this result from offset VSP data, we can more confidently assert that the polarization azimuth of the fast S-wave as determined from the near offset data correlates straightforwardly with formation properties.

The variations in S-wave polarizations of Figure 15 probably do not define a polarization pattern consistent with a

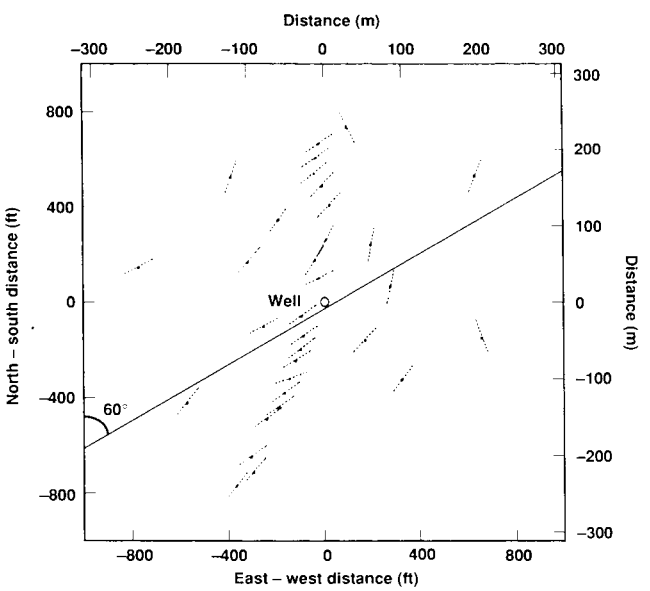

FIG. 13. Polarization azimuths of the fast S-waves from two concentric rings of offset VSPs around the Cymric well and a nearby walkaway VSP. Azimuths were determined by Alford rotation analysis with no layer stripping. The receiver was at a fixed depth of 1550 ft (472 m). Most azimuths are close to N 60°E, an indication that the upper zone dominates as it did at that depth for the near offset VSP (Figure 3a).

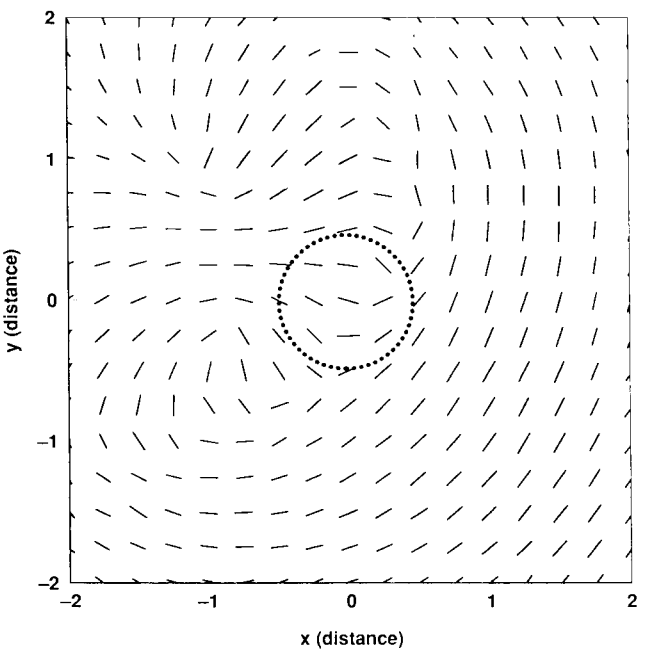

FIG. 14. Polarization pattern for the fast S-wave in a homogeneous solid with no vertical symmetry axis. Line segments show polarization directions that would be recorded on horizontal receiver components from surface sources offset laterally from the receiver by the indicated distances. Receivers are one distance unit vertically below the center of the plot. The dotted circle indicates source offsets of 700 ft (210 m) for a receiver at 1550 ft (470 m). The message is that, without a vertical symmetry axis, polarizations can vary with azimuth considerably even when source offset is small. With a vertical two-fold axis, any variation at small offsets would likely be small and would have two-fold symmetry. The anisotropic medium was synthesized by introducing vertical cracks parallel to the x-axis into a transversely isotropic matrix, where the infinite-fold axis of the matrix had been tilted 45 degrees from the vertical towards positive y and then rotated 28 degrees counterclockwise. (Compare Figure 5 of Paper I).

homogeneous medium, as they appeared to do at Lost Hills (see Paper I), but are probably effects of local inhomogeneities (possibly including topography) and of the inability of layer stripping in this area to obtain high precision with sparsely sampled offset VSP data. Partly for these reasons we did not attempt to model the polarizations with a homogeneous anisotropic model, and we did not have enough information to attempt an inhomogeneous model.

The inner ring.—The inner ring of offset VSPs with receiver at 1000 ft (305 m) was recorded to check robustness of *S*-wave polarization directions above the unconformity and also to allow comparison with results obtained below the unconformity. The consistency of the polarizations with the near offset result (Figure 16) indicates a robust environment for polarization analysis, but calculated lags, posted in the figure near the polarization bars, show considerable variability. The *S*-wave lag in near offset VSP data (Figure 3b) at 1000 ft (305 m) was 40.5 ms, larger than any in the inner ring offset VSP data.

Lag falls precipitously for the source located to the northeast of the well. The polarization of the neighboring deleted data point was approximately orthogonal to the others. It was rejected because it was the only point, during recording, for which the ARIS azimuth sequence was altered, and we assumed that its peculiarity resulted from faulty communication between the ARIS operator and the observer. Data quality was very good for all eight positions, but it was anomalously poor for two or three nearby positions of the outer offset rings, recorded at 1550 ft (472 m). This conjunction of unusual effects supports the possibility of a local anomaly to the east of the well.

Railroad Gap near offset VSP data

Figure 17 shows the *S*-wave wavelets of the 1700 ft (518 m) level of the near offset Railroad Gap VSP after rotating to minimize energy on off-diagonal components. There is considerable energy left on the off-diagonal components, but it is easy to identify the two *S*-waves on the diagonal components and note the large time delay between them. In surface reflection data, that 63 ms of lag would double to 126 ms, an amount sure to confuse any data analysis that did not take it into account.

Figure 18a shows the *S*-wave polarization azimuths relative to the source azimuth after the initial rotation analysis. As for the Cymric data (Figure 3a) the layer boundary is not evident in azimuth angle trends: The large lag that accumulated down to the bottom of the layer, in combination with a weakly birefringent zone below the layer, caused considerable inertia in azimuth angle determination. Below 2900 ft (880 m), however, the analysis indicates major changes in *S*-wave polarization directions. Directions indicated are contaminated by lags for the upper levels, however, and cannot be evaluated without eliminating that contamination.

As at Cymric, a change in lag trend (Figure 18b) clearly indicates where *S*-wave birefringence changes. The lag increases steeply down to 1300 ft (400 m) and then levels off below 1500 ft (460 m). Note that in the upper layer the slope of lag versus depth is approximately linear but that a fitted straight line would not pass through the origin, which is evidence of an anomaly in the very near surface. The lag

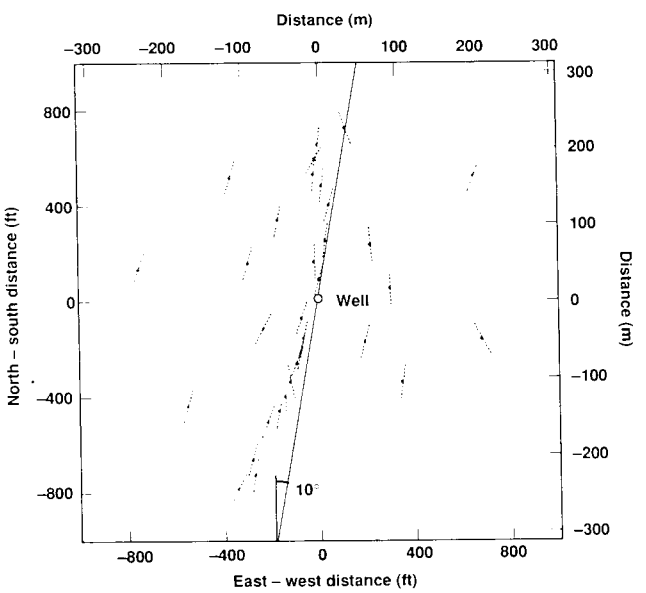

FIG. 15. Polarization azimuths like those of Figure 13 except that in this case azimuths were determined by Alford rotation analysis subsequent to a layer stripping in which the layer stripping static varied with source location (see text). The receiver was at a fixed depth of 1550 ft (472 m). Most azimuths are close to N 10°E, an indication that the offset VSP layer stripping worked and that *S*-wave polarizations at the various offset locations are consistent with the *S*-wave polarization from near offset data.

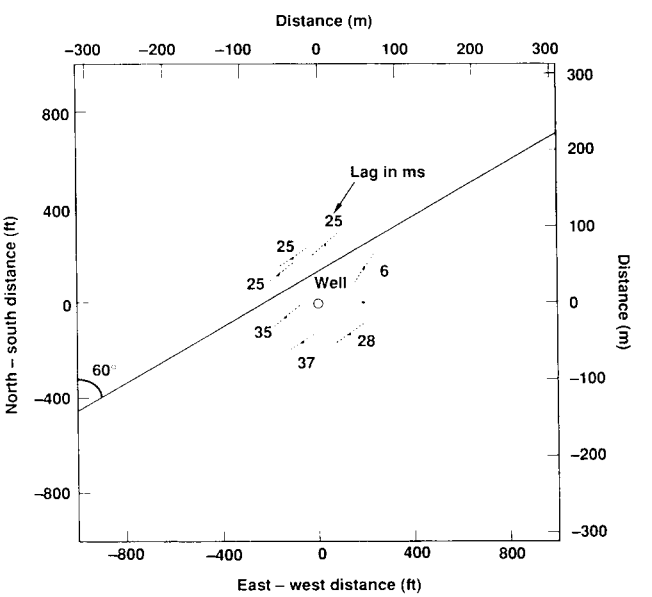

FIG. 16. Polarization azimuths of the fast *S*-waves after Alford rotation from a ring of offset VSPs around the Cymric well. The receiver was at a fixed depth of 1000 ft (305 m). Most azimuths are close to N 60°E, consistent with the near offset VSP result for that depth. The deleted azimuth was approximately orthogonal to the others, probably because of a recording error (see text).

from the 100 ft (30 m) level is anomalous, as was the case also in Lost Hills (Paper I) data. At Cymric, lags from the uppermost 350 ft (110 m) were anomalous (Figure 3b).

Seven layers were needed to accommodate all *S*-wave polarization changes. Figures 19 and 20 summarize final azimuth angle and lag results, respectively, for all seven layers. All lag trends except those of layer 3 show a smooth, monotonic increase with depth, as assumed by the layer stripping model (see Paper I). Layer 3 is less birefringent than other layers for vertically traveling *S*-waves, and the associated azimuth angles show correspondingly large scatter, inspiring little confidence in the analyses for that layer.

Superposed on Figure 19 are azimuth angles determined from layer stripping under the assumption of only three layers down to 6500 ft (1980 m). The dotted lines indicate azimuth trends for the two deeper layers. This comparison shows that, even if layer boundaries are not chosen with scrupulous care, the answers obtained in the thicker and more highly birefringent depth zones can still be close to the correct ones. The layer stripping process, in short, is robust.

Layer stripping often improves the quality of *S*-wave data recorded below polarization changes, as we noted for the Lost Hills (Paper I) and Cymric (above) data, but improvement was especially noticeable in Railroad Gap data. Leading portions of X'X' and Y'Y' *S*-wave wavelets of Figure 17 have relatively similar shapes. Their counterparts from data recorded at greater depths, however, were dissimilar after the first Alford rotation. Layer stripping followed by further Alford rotations significantly increased the similarity. Figure 21 compares diagonal *S*-wave wavelets after the first Alford rotation with diagonal *S*-wave wavelets from the same depths after the fourth layer stripping, down to 3700 ft (1130 m). Improvements from layer stripping are obvious. The off-diagonal components (Figure 22) also have appreciably less energy in the analysis time window after layer stripping than before.

Improvements such as these were easy to make in the VSP data, but, as food for thought, we note that surface reflection seismic data would be more severely affected than VSP data, and proper corrections appreciably more difficult. Corrections of surface data may often require aid from VSP data.

DISCUSSION

Salient features in the birefringence analyses of near offset Cymric and Railroad Gap VSP data are (1) the large magnitudes of the vertical *S*-wave birefringence in the uppermost layers followed by diminished birefringence at greater

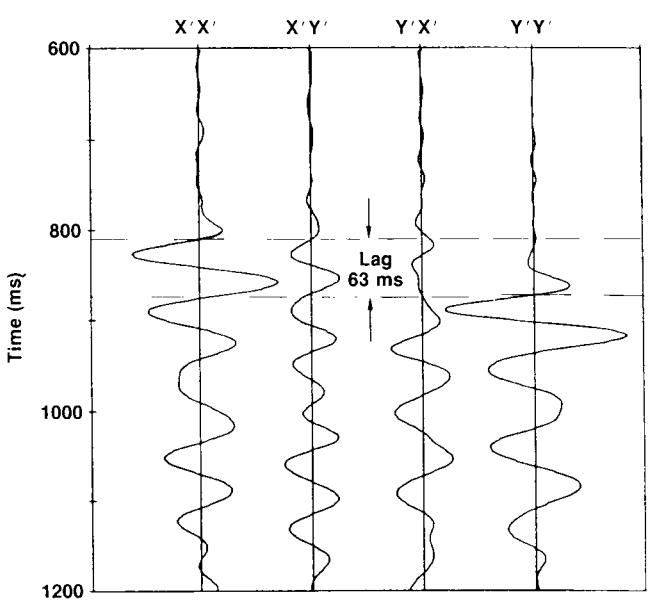

FIG. 17. 2 × 2 *S*-wave data matrix from the 1700 ft (518 m) level of the Railroad Gap VSP after rotation to minimize energy on off-diagonal (X'Y' and Y'X') components. The lag of 63 ms was determined by crosscorrelation.

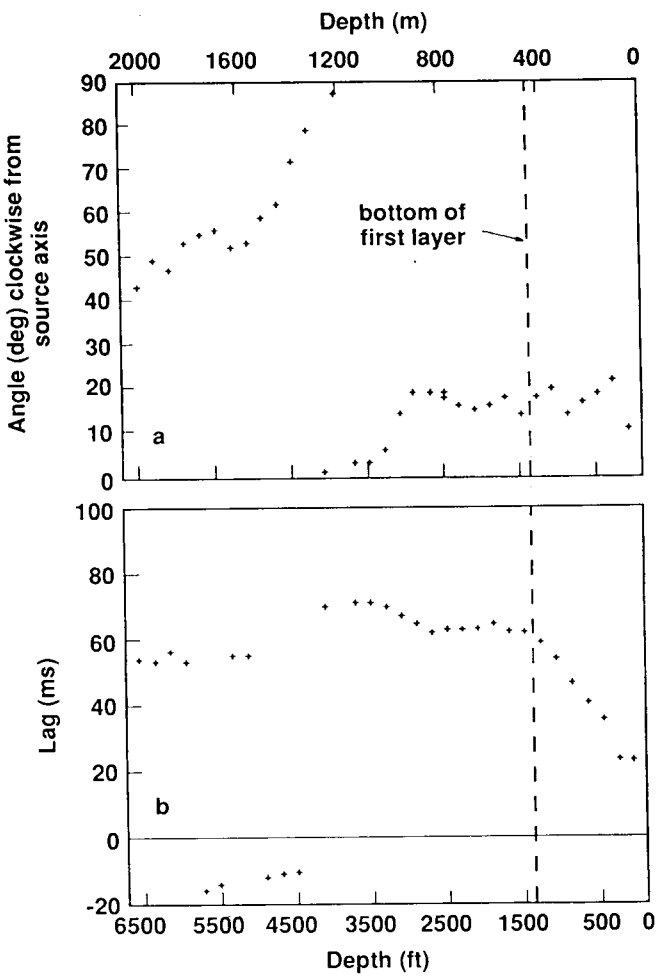

FIG. 18. a) Polarization azimuths of the fast *S*-wave relative to the ARIS source axis as determined from the initial Alford rotation analysis of Railroad Gap VSP data, before any layer stripping. Angles are consistent down to 2900 ft (880 m), an effect of inertia in azimuth angle determination resulting from the large accumulated lag between the *S*-waves (see Figure 17). b) Lags between *S*-waves of the Railroad Gap VSP after the initial Alford rotation analysis but before any layer stripping. Above 1300 ft (400 m) the *S*-wave birefringence reaches 9 percent. The abrupt change of slope near 1500 ft (460 m) indicates a change in *S*-wave birefringence and signals a change in *S*-wave polarization, discovered by layer stripping and subsequent Alford rotation analysis.

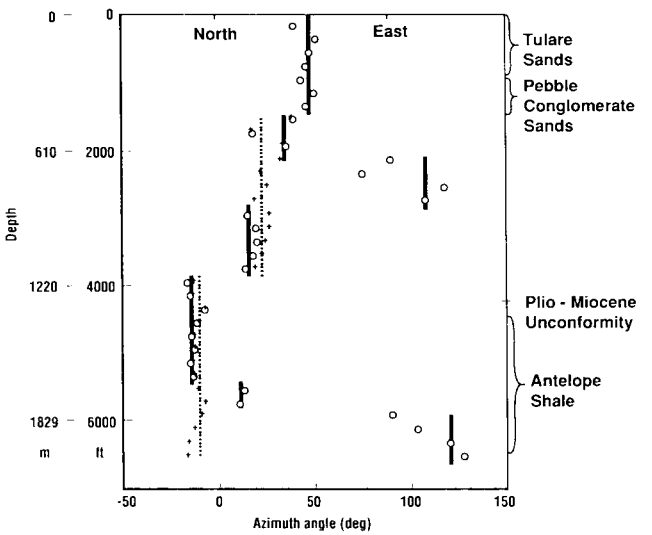

FIG. 19. Summary of polarization angles of the fast *S*-wave versus depth for the Railroad Gap VSP data. Seven layers were needed to accommodate changes in *S*-wave polarization (circles and solid vertical bars). Layer stripping was also done with only three layers (plusses and dotted vertical bars) to evaluate magnitudes of errors likely to result from less conscientious layer stripping. The first layer was the same for both layer stripping sequences.

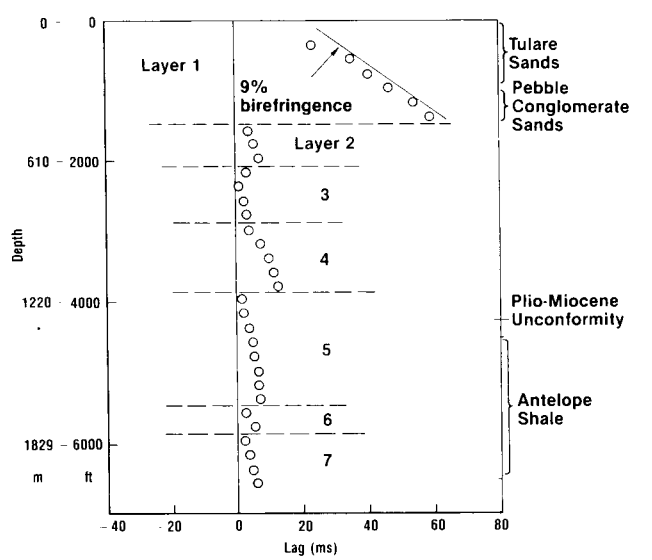

FIG. 20. Summary of *S*-wave lag versus depth for the Railroad Gap VSP data. Vertical *S*-wave birefringence was unusually large in Layer 1 and decreased in deeper layers. Lags increased monotonically in every layer but one.

depths and (2) the changes of *S*-wave polarization azimuth with depth. Neither feature had been anticipated, but both add greatly to the interest and potential significance of the data.

Magnitudes of S-wave birefringence

The large magnitudes of the vertical *S*-wave birefringence are of interest in themselves because of their value in helping to establish norms at this early stage of anisotropy investigation. Typical values of vertical *S*-wave birefringence in sedimentary basins were thought to have been less than 4 percent (Winterstein, 1987). Recently, Brodov et al. (1990) reported 3, 7, and 15 percent in reservoir rock monitored by three closely spaced VSPs recorded at the Romashkino field. Their figures unfortunately were flawed. A second look at the data suggests 12 to 20 percent, but we await their revised estimates. Becker et al. (1990) reported 6 to 8 percent in fractured Austin chalk at Marcelina creek; but their data appear to need layer stripping and reinterpretation. Majer et al. (1988) reported 11 percent *S*-wave birefringence in offset VSP data from The Geysers geothermal field, but their raypaths were at large angles (about 45 degrees) from the vertical. Large *S*-wave birefringence in directions appreciably different from the vertical does not necessarily imply vertical *S*-wave birefringence (cf. Winterstein and Paulsson, 1990). Also, their offset VSP data were not sampled uniformly along the raypaths, so that changes in *S*-wave polarization direction between source and receiver might have gone undetected. Recently, they reinterpreted the large

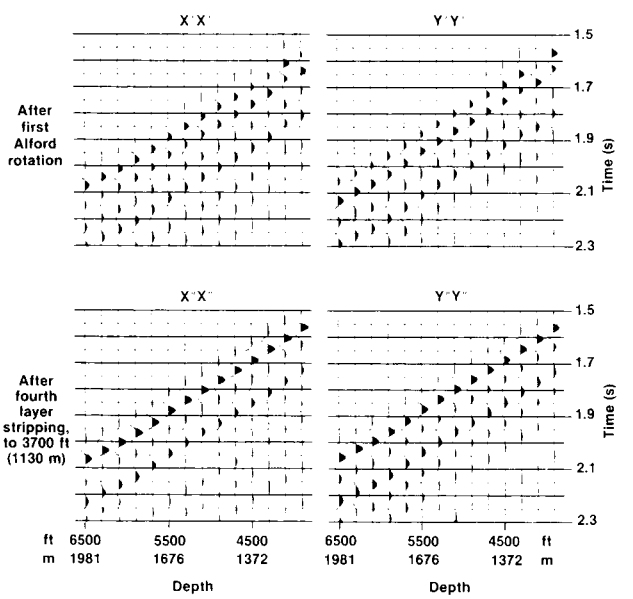

FIG. 21. Diagonal components of the 2 × 2 *S*-wave data matrix from Railroad Gap Layers 5 through 7. Upper plots show data after the first Alford rotation but before any layer stripping. Lower plots show data after the Alford rotation following the fourth layer stripping, to 3700 ft (1130 m). Leading portions of wavelets on XX components are more similar to their counterparts on YY components after layer stripping than before, an indication that layer stripping caused a better fit to the seismic model. Wavelets are also more consistent with depth than before.

difference in S-wave arrival times as an effect of P-S conversion instead of anisotropy (Campden et al., 1990). Lynn (1989) showed data recorded by Redpath and associates that clearly document vertical S-wave birefringence of 12 percent at Livermore, California, but measurements extended to only 200 ft (61 m) below the surface. Measurements presented here show obvious S-wave birefringence, in one case up to 14 percent, along nearly vertical raypaths from depths of 100 to 1550 ft (30 to 470 m) (Cymric) or to 6500 ft (1980 m) (Railroad Gap). The increase in S-wave splitting across a given anisotropic layer can be monitored visually by comparing actual S-wave wavelets after Alford rotations. For brevity only the wavelets of Figures 2 and 21 are shown explicitly, but lags from S-wave crosscorrelations are given in detail for all depths (Figures 3b, 7, 10, 18b, and 20).

For deducing causes of anisotropy it is noteworthy that the largest vertical S-wave birefringence in both the Cymric and Railroad Gap fields occurred in the same formations, the Pliocene Tulare sandstone and San Joaquin Pebble Conglomerate sandstone. The Tulare is described by geologists working the oil fields as a dirty, poorly sorted sandstone with high feldspar content. Constituent sizes run from fine grains to cobbles, and there are several interbedded shales. Pore fluid is air down to 475 ft (145 m) at Cymric and down to 650 ft (200 m) at Railroad Gap. The Pebble Conglomerate is a true conglomerate with diatomite clasts. Below these formations birefringence tended to diminish appreciably in both fields (Figures 10 and 20).

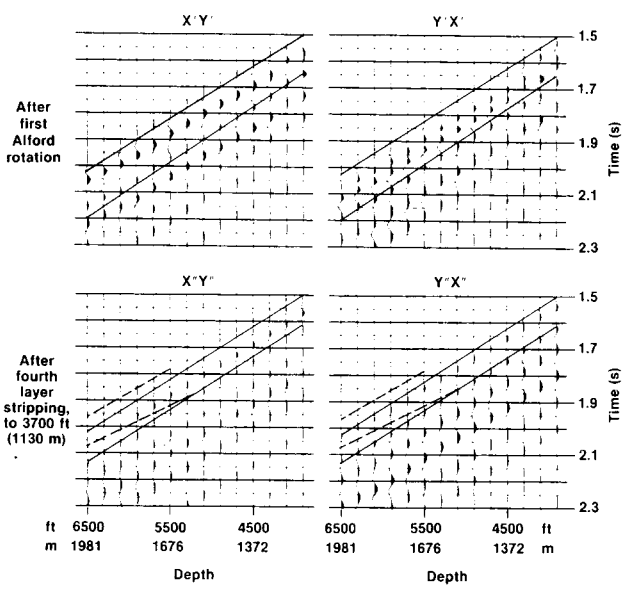

FIG. 22. Off-diagonal components of the 2 × 2 S-wave data matrix from Railroad Gap Layers 5 through 7. Upper plots show data after the first Alford rotation but before any layer stripping. Lower plots show data after the Alford rotation following the fourth layer stripping, to 3700 ft (1130 m). Analysis windows are indicated by diagonal lines. Wavelet amplitudes in the analysis windows are lower after layer stripping than before, an indication that layer stripping caused a better fit to the seismic model. Both the dashed and the solid analysis windows were used for the two deepest layers. Consequences of using the different windows were negligible.

Although firm conclusions about models cannot be drawn from existing data, the large vertical S-wave birefringence at small depths followed by diminished birefringence at greater depths is more consistent with the Nur model than with extensive dilatancy anisotropy (EDA). (See Introduction, Paper I, for discussion of Nur and EDA models.) EDA cracks open perpendicular to the direction of minimum compressive stress. At sufficiently shallow depths the minimum stress should be vertical and any EDA cracks horizontal. Resulting anisotropy would be TI (transversely isotropic) with a vertical symmetry axis, a symmetry system for which there is no vertical S-wave birefringence. For the Nur model, on the other hand, a large horizontal stress in one direction coexisting at small depths with a small horizontal stress orthogonal to it and a small vertical stress would close Nur model cracks in one direction only and tend to yield the largest possible vertical birefringence. With increasing depth all three stresses increase, closing Nur model cracks in all directions and leaving rocks weakly anisotropic. Nur model cracks in formations such as the Tulare probably are not true cracks but randomly oriented pore throats of small aspect ratio. As stresses increase, such pore spaces oriented perpendicular to the maximum compressive stress will close preferentially. The large effects at small depths also suggest that in these sedimentary rocks, magnitudes of rock compliances are more important than magnitudes of in-situ stresses as causes of large S-wave birefringence.

Changes in S-wave polarization direction with depth

Possible correlation with stress directions: Cymric.—We have documented major changes in S-wave polarization direction with depth, but the reasons for the changes are not clear. The most important question is whether the polarization changes correspond to changes in horizontal stress direction or whether they simply indicate changes in preexisting cracks or other structures. Information on in-situ stress directions is sketchy at best for both oil fields, but what data are available at Cymric suggest that the polarization direction of the fast S-wave parallels the direction of maximum horizontal stress below the unconformity at about 975 ft (300 m). The fast S-wave polarization direction there is roughly N 10°E.

A test conducted 1500 ft (460 m) north of the Cymric VSP well indicated the direction of maximum horizontal stress, or natural fracture orientation, was N 7°E below the unconformity. This test was a cyclic steam flood in which steam injected in one well (1704S) was monitored in two nearby wells (1704O and 1704D). One of the monitor wells (1704O) was 23 ft (7 m) away along an azimuth of N 7°E, while the other was 19 ft (6 m) west of the 1704O. Temperatures in the first monitor well rose within a few hours of steam injection, indicating a direct conduit between injector and monitor wells. Temperatures in the second monitor well, however, remained unchanged over a period of months. From the temperature distribution in the first monitor well it was apparent that the steam conduit was about 75 ft (20 m) high and nearly vertical at depths in the 1050–1150 ft (320–350 m) range. Antelope shale below the unconformity is known to

be naturally fractured, but fracture orientation is unknown. Engineers working the reservoir believe that steam opens fractures along the direction of maximum horizontal compressive stress. If so, the steam injection test indicates that the direction of maximum horizontal stress below the unconformity is along N 7°E, in good agreement with the angle determined from *S*-wave VSP data.

Further corroboration of a northerly direction of maximum horizontal stress below the unconformity comes from tiltmeter data recorded during hydraulic fracturing in the 1116S well located in the adjacent section to the east. Tiltmeter data analysis concluded that hydraulic fracturing at a depth of 2300 ft (700 m) created a nearly vertical fracture striking N 7°W ± 7°. This tiltmeter result was obtained after compensating for a point loading force calculated to have been exerted on the surface, and subsequently removed, by fluid and proppant injected during the fracturing. The tiltmeter result is somewhat suspect because the compensation for surface loading was not routine and probably would not have been done if initial answers had not indicated a horizontal fracture. However, calculations showed that the surface loading was important, and we have no reason to dispute subsequent analysis results, other than on the usual grounds of an overly simple model. Because of the unconformity and structural complexity, the usual homogeneous model may have been particularly inappropriate at Cymric.

Finally, a detailed study by Hansen and Purcell (1986) based on analysis of tiltmeter data and wellbore breakouts determined that the direction of maximum horizontal stress in the South Belridge field about 7 mi (11 km) to the north was N 15°E ± 15° at reservoir depths. Although 7 mi (11 km) is too great a distance to inspire confidence in correlations of stress directions, it is not so far as to be irrelevant because, as we shall see, the *S*-wave polarization azimuths at Railroad Gap 4.5 mi (7.2 km) to the southeast correlate with those at Cymric. The Belridge studies were done in a Miocene formation, the Belridge diatomite, which is somewhat younger than the Antelope shale at Cymric but older than the rocks above the Plio-Miocene unconformity. Comparison of Cymric and Railroad Gap results suggests that, in this geographic locality, relative position in the stratigraphic column correlates better with *S*-wave polarization directions than absolute depth of burial.

Analysis of offset VSP data combined with information presented above supports interpreting the polarization direction of the fast *S*-wave in near offset data as the direction of maximum horizontal stress despite the large dip of the deeper beds. Above the unconformity at Cymric, bedding is relatively flat, consistent with the VSP well's location near the crest of a broad anticline. Below the unconformity, however, bedding tilts about 35 degrees to the southwest. If anisotropy symmetries tilt similarly, even if there are oriented vertical cracks or a well-defined direction of maximum horizontal stress, it is possible that the polarization direction of the fast *S*-wave may be uncorrelated with the crack or stress direction (see Figures 14; also, Figure 5 of Paper I). Hence the ability to layer strip the offset VSP data and come up with *S*-wave polarization directions that are consistent with those of the near offset VSP (see above) was important. Modeling suggests that, if *S*-wave polarizations of offset VSP data agree with those of zero offset data when anisotropy has low symmetry, then there is likely to be a near vertical symmetry axis or "pseudo symmetry axis"; and in relatively simple cases, polarization of the fast *S*-wave will be oriented along the direction of fracture strike or of maximum horizontal stress. By pseudo symmetry axis we mean that the medium does not have a true vertical symmetry axis but is so close to having one that it behaves almost as though it did. The monoclinic medium used to model Lost Hills data (Figure 22 of Paper I) had such an axis.

The Cymric near offset VSP data show that the polarization direction of the fast *S*-wave changes from roughly N 60°E in the uppermost 800 ft (240 m) to roughly N 10°E from 1050–1550 ft (320–470 m). This change, in view of the foregoing, suggests that the direction of maximum horizontal stress rotated about 50 degrees to the north below the unconformity.

Possible correlation with stress directions: Railroad Gap.— Efforts to determine in-situ stress directions independently at Railroad Gap involved anelastic strain recovery (ASR) measurements, differential strain curve analyses (DSCA) and FMS log analysis. Scatter was too large in ASR results to warrant taking them seriously, but the DSCA results were more consistent. For the most part, they disagreed by substantial amounts, up to 60–80 degrees at some depths, with the polarization azimuths of the fast *S*-waves. We do not consider DSCA answers conclusive, as they are subject to many sources of systematic error. The DSCA method requires that a sample in the shape of a cube be cut from a core, fit with strain gauges, and subjected to large hydrostatic stresses. Downhole in-situ stresses are inferred from strains induced in this manner in the laboratory. Many assumptions are required to interpret the data, not the least of which is that the former subsurface sample orientation is known. Analysis of FMS log data from the Railroad Gap VSP well also proved inconclusive.

Hence at the moment, we cannot affirm confidently any correlation of stress direction with *S*-wave polarization direction at Railroad Gap (Figure 19). However, other considerations suggest a correlation. Ignoring the weakly birefringent third anisotropic layer (Figures 19 and 20) and interpreting with a broad brush, we note that the trend in azimuth of the fast *S*-wave polarization down to about 5300 ft (1620 m) is somewhat like that at Cymric. The highly birefringent zone in the Tulare and Pebble Conglomerate sands at Railroad Gap extends down to 1300 ft (400 m) versus 800 ft (240 m) at Cymric, and the Plio-Miocene unconformity at 4250 ft (1300 m) is also much deeper than at Cymric (975 ft [300 m]). If *S*-wave polarization directions are considered in terms of formations instead of depths, the pattern of *S*-wave polarization changes at Railroad Gap thus appears remarkably similar to that at Cymric. The fast *S*-wave polarization azimuth in the uppermost anisotropy layer at Railroad Gap is N 46°E versus N 60°E at Cymric. Average azimuth in the next zone of well-defined *S*-wave birefringence, namely, that from 2900–3700 ft (880–1130 m) is N 16°E, while that in the deepest zone of well-defined birefringence, namely, from 3900–5300 ft (1190–1610 m) is N 15°W. The difference in fast *S*-wave azimuth angle between the Tulare sandstone and the Antelope shale is hence about 61 degrees at Railroad Gap and 50 degrees at Cymric. Thus,

S-wave polarization directions and possibly also stress directions for a given subsurface formation are simply rotated 15–25 degrees counterclockwise at Railroad Gap field relative to what they are at Cymric.

This similarity in *S*-wave polarization changes with depth at Cymric and Railroad Gap supports the likelihood that *S*-wave polarization directions are determined by stress directions. That is, if stress determines *S*-wave polarizations in one of the two areas, for example, Cymric, then the similarity in behavior suggests that it does so for both.

Stress variations with depth and the San Andreas fault.—The reasons for the changes of fast *S*-wave polarization direction with depth at Cymric and Railroad Gap are unknown, but at Cymric the proximity to the Plio-Miocene unconformity, a major angular unconformity, is suggestive. Hickman et al. (1988) observed analogous changes in stress direction over a 500–900 ft (180–270 m) interval in the Hi Vista well located in a similar position relative to the San Andreas fault. They point out that rapid variations of stress magnitude and direction with depth have been observed elsewhere but have seldom been adequately explained. They suggest that a major stratigraphic discontinuity or slip on a fault might abruptly change stress magnitude or orientation. A recent study of wellbore breakouts of the Cahon pass scientific well indicated large variations of maximum horizontal stress direction with depth (M. D. Zoback, pers. comm., 1990).

A way conceptually to tie together the major *S*-wave polarization trends of the Cymric and Railroad Gap fields, although speculative, is to view them in terms of stresses on the San Andreas fault. The San Andreas fault runs NW–SE about 10 mi (16 km) southwest of the two VSP sites. Zoback et al (1987) cite evidence that maximum horizontal compressive stress tends to be perpendicular to the fault in central California, and they propose a model involving convergent plate motion to account for such "fault-normal compression." Ordinarily, stresses associated with a vertical strike-slip fault plane would cause maximum horizontal compression at an angle of 30–45 degrees from the fault strike (Zoback et al., 1987). If the *S*-wave polarization azimuths are telling us stress direction, then they indicate maximum horizontal compression nearly orthogonal to the San Andreas at small depths, consistent with the Zoback et al. (1987) model. But at greater depths, in the Antelope shale formation, maximum compression is more like 45 degrees from the fault strike, consistent with the conventional strike-slip model. Possibly, as stress builds up before rupture, deeper compressive stresses in close proximity to the fault become aligned in directions conducive to strike-slip motion along the fault. Anticlinal structures parallel to the fault indicate that fault-normal compression historically has extended to greater depths than the Antelope shale, but such compression may vary with time and depth and depend strongly on space-time proximity to rupture along the fault.

Further VSP measurements of *S*-wave birefringence will give a clearer picture than we now have of the variability of subsurface velocity anisotropy in tectonically active areas, and from these it should be possible to formulate good theories of causes.

Accuracy of fine layer stripping.—Refining the layer stripping to resolve polarization directions in ever thinner layers raises questions of accuracy and believability: At what point does noise or systematic error dominate results? Can we believe the polarization change indicated, for example, at 1450–1500 ft (440–460 m) in the Cymric data of Figure 9? The question is multifaceted. We have no hard answers at this early stage of investigation, but we do have insight into relevant variables. Accuracy depends strongly on how carefully the data are recorded, the method of data analysis, signal-to-noise ratios, and the magnitude of the birefringence. If there is no birefringence in a given layer, there is no natural polarization direction, and any determination of it is spurious. Hence, results from strongly birefringent layers inspire greater confidence, all else being equal, than those from weakly birefringent layers. Also, while most analysis methods become unstable under one set of circumstances or another (e.g., Winterstein, 1989), the Alford rotation method seems to be robust in most cases, provided that S/N is reasonably good and that it is possible to do the layer stripping properly. Furthermore, we have found that when we attempt to layer strip at every depth level, in some instances answers fluctuate wildly.

One reason it is not possible to provide hard answers to the question of accuracy is that, ultimately, the quality of the data dominates. If we were able to generate identical source wavelets every shot and record them in a noise-free environment, answers would often be valid down to lags of fractions of a millisecond. We assert this because in some cases lags vary smoothly from one depth to the next by amounts as small as a millisecond (see Figure 20 and Figure 15 of Paper I). If lags show a lot of scatter, of course, as they did in the ARCO Group Shoot data (e.g., Cox et al., 1989), detailed analysis is impossible. But whether or not lags show scatter depends strongly on recording practice. Changing the source or its location in any way, for example, seems to be a serious offense.

The reason we believe the erratic polarization answers at 1450–1500 ft (440–460 m) in the Cymric analysis is that the *S*-wave lags there persistently followed a trend that contrasted with neighboring lags. In the preceding layer stripping steps, they dropped when the others rose, and by amounts that seemed larger than the scatter in the lags. However, we are not confident enough of those answers to base a major decision on them, because it is possible that they result from unknown sources of systematic error. Furthermore, the birefringence in that thin layer is small.

Reasons to believe the divergent answers at the unconformity (900–1000 ft, 275–305 m), are 1) the unconformity itself is a reason for expecting unusual behavior, 2) the lags are of significant magnitude and 3) the fine layer stripping causes the lags to fit the layer stripping model in a way they did not fit under the two-layer assumption. That is, in the initial layer stripping those lags near the top of the second layer did not show a monotonic increase but were anomalously large (Figure 7).

A feature of fine layer stripping worth mentioning is the tendency of answers to converge upon downward continuation. In every case so far, layer stripping done with two different angles and lags at a shallow level gives answers that disagree by larger amounts at the shallow level than they do

after downward continuation to deeper levels (cf. Figure 9). This behavior suggests that errors in initial analyses do not propagate into subsequent analyses but instead tend to vanish. A possible reason is that wave propagation in a deeper layer if continued long enough would eventually cause the two *S*-waves to separate enough so that polarization analysis would tend to give correct answers regardless of what happened above (see Figures 12, 23, 24 in Paper I and associated discussion). In other words, if layers were thick enough and sufficiently birefringent, we would tend to get correct answers near layer bottoms even without layer stripping. The observation of answers converging at depth is tempered, however, by our further observation that multiple layer strippings at small depth increments at Cymric caused apparent deterioration in data quality at the deepest levels.

In the Railroad Gap analyses we can justify dismissing or at least downgrading answers from the third layer because of the weak birefringence (Figure 20), but the seventh layer shows a well-behaved increase in lag with depth and thus cannot be easily dismissed. There is a change in subsurface structure at about 6000 ft (1830 m) that might lead us to expect a change in *S*-wave polarization. Specifically, dipmeter analysis reveals that dip increases gradually over the interval 4500–5960 ft (1370–1820 m) from 10 degrees to 20 degrees, with beds dipping towards the southwest. Abruptly between 5960 and 6000 ft (1820 and 1830 m) the dip changes to 50 degrees to the northeast. By 6200 ft (1890 m) it comes back to 30 degrees to the southwest. Such changes may be associated with faulting and also a change in stress direction.

In the case of the seventh layer at Railroad Gap, energy on the off-diagonal components was very small after Alford rotation following the fourth layer stripping (Figure 22) and was imperceptibly different by eye from that after the sixth layer stripping, and the azimuth angles were comparable to those of the fifth layer (possibly because of inertia—see dotted line of Figure 19). However, after the fourth layer stripping the lags from 3900–6500 ft (1190–1980 m) were inconsistent with a homogeneous anisotropic model. Specifically, lags increased monotonically to 9.3 ms at 5700 ft (1740 m), then dropped to 7.7 ms at 6100 ft (1860 m). Although this drop is small by ordinary standards of seismic data analysis, it contrasted markedly with the overall lag trend and hence suggested that further layer stripping was needed. Also, random scatter appeared negligible. The change in lag trend was analogous to that shown in Figure 15 of Paper I below 700. ft (210 m). Consequently we stripped off two more layers, at 5300 and 5700 ft (1620 and 1740 m) and obtained results that are consistent with the layer stripping model. The high quality of data after layer stripping supports expectations of high accuracy (see Figure 21).

CONCLUSIONS

We have shown clear examples of large vertical *S*-wave birefringence in carefully recorded VSP data from the uppermost 1550 ft (470 m) of sedimentary rock in the Cymric oil field and the uppermost 6500 ft (1980 m) in the Railroad Gap field. The birefringence is obvious because lags between the two *S*-waves increase monotonically over several depth zones, and the increase in lag is visually evident in plots of data after applying Alford rotations. Magnitudes of vertical *S*-wave birefringence reached 14 percent at Cymric and 9 percent at Railroad Gap in the uppermost formations, the Pliocene Tulare and Pebble Conglomerate sands. Below those formations, birefringence dropped to more typical values (<4 percent), but stayed above 6 percent in the opal A zone of the Antelope shale at Cymric. Large vertical *S*-wave birefringence near the surface favors the Nur model over EDA, although not definitively, as a possible mechanism.

Near offset VSP data from both oil fields show unmistakable evidence of major changes in *S*-wave polarization directions with depth. Abrupt changes in the slope of *S*-wave lag versus depth initially suggested the presence of polarization azimuth changes. Such changes were detected and analyzed by means of a simple layer stripping process. Refined layer stripping showed that not all polarization changes are signaled by a noticeable change either in the slope of the lag curve or by changes in azimuth angles, but must be detected by layer stripping at arbitrary points.

Independent evidence that polarizations of the fast *S*-wave were oriented along the direction of maximum horizontal compressive stress is much less compelling at Cymric and Railroad Gap oil fields than it was at Lost Hills field (Paper I), but what evidence there is at Cymric supports a correlation. There is no corroborating evidence yet at Railroad Gap, but similarities in polarization azimuths with depth to those at Cymric suggest that, if maximum horizontal stresses correlate with fast *S*-wave polarization directions at Cymric, they should also do so at Railroad Gap. Somewhat speculative evidence of a connection between stress and *S*-wave polarization comes from the proximity of the San Andreas fault. Zoback et al. (1987) point out that maximum horizontal compressive stress is normal to the fault strike in this part of California. We observe fast *S*-wave polarization directions approximately normal to the fault in both areas in the Pliocene Tulare and Pebble Conglomerate formations. Deeper, in the Antelope shale, the fast *S*-wave polarization is closer to 45 degrees from the fault, consistent with a stress environment that would cause strike-slip motion along the fault. More research is needed to pin down any correlation of stress with *S*-wave polarization, but available evidence suggests such a correlation.

The layer stripping procedure enabled us to evaluate accurately the variations in *S*-wave birefringence with depth. *S*-wave polarization azimuths of a given anisotropic layer were generally consistent over hundreds of feet, a property that fits nicely with assumptions of the layer stripping model. We have not compared layer stripping with the transfer function method (Lefeuvre et al., 1989; Cox et al., 1989), but it would clearly be of great interest to do so for these VSP data sets. Besides clarifying data interpretation, the layer stripping caused data after rotation analysis to comply better with expectations from simple anisotropic models. This, and obvious improvements in *S*-wave data quality after layer stripping, bolstered our confidence in its validity.

Layer stripping of offset VSP data with lags individually tailored to each source location effectively allowed us to see below the uppermost anisotropic layer in offset data at Cymric. Resulting *S*-wave polarizations were consistent with the *S*-wave polarization of the second layer as calculated from the near offset VSP. The consistency suggests the

presence of a near vertical symmetry axis or pseudo symmetry axis like the one at Lost Hills (Paper I).

ACKNOWLEDGMENTS

We thank those who aided with planning and data acquisition, especially Clint Frasier, who suggested the offset VSP configuration as a check on interpretability of near offset VSP data. We thank also Paul Donoho and John Fairborn, who made the MicroMAX accessible as a useful field computer, and numerous others, both in Chevron operating companies and at Chevron Oil Field Research Company, without whose timely help the experiments could not have been successfully completed. Bharat Gael's enthusiastic consultation and support were extraordinarily helpful, and M. Kumar, Louis Klonsky, Gena Evola, and Jerry Kennedy provided important background information. Indispensable operational support was provided in the field by Randy Dickey, Blake Loke, Larry Neal, and Steve Wilcox. We thank Chevron Oil Field Research Company for supporting the research and for permission to publish.

REFERENCES

Alford, R. M., 1986, Shear data in the presence of azimuthal anisotropy: Dilley, Texas: 56th Ann. Internat. Mtg., Soc. Explor. Geophys., Expanded Abstracts, 476–479.

Becker, D. F., Bishop, G. L., Clayton, K. N., Peterson, D. N., Rendleman, C. A., and Shah, P. M., 1990, Shear-wave anisotropy at Marcèlina creek: SEG workshop: Vector Wave Field Seismology Update, San Francisco.

Brodov, L., Kuznetsov, V., Tikhonov, A., Cliet, Ch., Marin, D., and Michon, D., 1990, Measurements of azimuthal anisotropy parameters for reservoir study: Fourth International Workshop on Seismic Anisotropy, Edinburgh.

Campden, D. A., Crampin, S., Majer, E. L., and McEvilly, T. V., 1990, Modeling the Geysers VSP: A progress report: The Leading Edge, **9**, 36–39.

Cox, V. D., Rizer, W. D., Anno, P. D., and Queen, J. H., 1989, An integrated study of seismic anisotropy and the fracture system in the Spraberry sandstone, Pembrook, field, Upton and Reagan Counties, Texas: Presented at the SEG Summer Research Workshop on Recording and Processing Vector Wave Field Data, Snowbird, Utah.

Hansen, K. S., and Purcell, W. R., 1986, Earth stress measurements in the South Belridge oil field, Kern County, California: SPE 15641, 1–15.

Hickman, S. H., Zoback, M. D., and Healy, J. H., 1988, Continuation of a deep borehole stress measurement profile near the San Andreas fault: 1. Hydraulic fracturing stress measurements at Hi Vista, Mojave Desert, California: J. Geophys. Res., **93**, 15183–15195.

Lefeuvre, F., Cliet, C., and Nicoletis, L., 1989, Shear-wave birefringence measurement and detection in the Paris basin: 59th Ann. Internat. Mtg., Soc. Explor. Geophys., Expanded Abstracts, 786–790.

Lynn, H. B., 1989, Field measurements of azimuthal anisotropy: First 60 meters, San Francisco Bay area: Presented at the SEG Summer Research Workshop on Recording and Processing Vector Wave Field Data, Snowbird, Utah.

Martin, M. A., Davis, T. L., and O'Rourke, T. J., 1986, An integrated three-component approach to fracture detection: 56th Ann. Internat. Mtg., Soc. Explor. Geophys., Expanded Abstracts, 235–236.

Majer, E. L., McEvilly, T. V., Eastwood, F. S., and Myer, L. R., 1988, Fracture detection using *P*-wave and *S*-wave vertical seismic profiling at The Geysers: Geophysics, **53**, 76–84.

Winterstein, D. F., 1987, Shear waves in exploration: A perspective: 57th Ann. Internat. Mtg., Soc. Explor. Geophys., Expanded Abstracts, 638–641.

——— 1989, Comparison of three methods for finding polarization direction of the fast shear wave: Presented at the SEG Summer Research Workshop on Recording and Processing Vector Wave Field Data, Snowbird, Utah.

Winterstein, D. F., and Meadows, M. A., 1991, Shear-wave polarizations and subsurface stress directions at Lost Hills field: Geophysics, **56**, 1331–1348.

Winterstein, D. F., and Paulsson, B. N. P., 1990, Velocity anisotropy in shale determined from crosshole seismic and VSP data: Geophysics, **55**, 470–479.

Yardley, G., and Crampin, S., 1990, Automatic determination of anisotropic parameters from shear-wave splitting in the Lost Hills VSP: Presented at the 60th Ann. Internat. Mtg., Soc. Explor. Geophys.

Zoback, M. D., Zoback, M. L., Mount, V. S., Suppe, J., Eaton, J. P., Healy, J. H., Oppenheimer, D., Reasenberg, P., Jones, L., Raleigh, C. B., Wong, I. G., Scotti, O., and Wentworth, C., 1987, New evidence on the state of stress of the San Andreas fault system: Science, **238**, 1105–1111.